Published in Applied Physics B: Lasers and Optics 75, issues 2-3, 351-357, 2002
which should be used for any reference to this work

Chemical sensing with pulsed QC-DFB lasers operating at 15.6 μm

A.A. KOSTEREV[1,✉] R.F. CURL[1] F.K. TITTEL[1] M. ROCHAT[2] M. BECK[2] D. HOFSTETTER[2] J. FAIST[2]

[1] Rice Quantum Institute, Rice University, Houston, TX 77251-1892, USA
[2] Physics Institute, University of Neuchâtel, Breguet 1, 2000 Neuchâtel, Switzerland

ABSTRACT Pulsed thermoelectrically cooled QC-DFB lasers operating at 15.6 μm were characterized for spectroscopic gas sensing applications. A new method for wavelength scanning based on repetition rate modulation was developed. A non-wavelength-selective pyroelectric detector was incorporated in the sensor configuration giving the advantage of room-temperature operation and low cost. Absorption lines of CO_2 and H_2O were observed in ambient air, providing information about the concentration of these species.

PACS 42.62.-b; 82.80.Gk; 82.80.Ha

1 Introduction

Quantum cascade (QC) laser technology has made a significant advance since its first introduction by Capasso et al. in 1994 [1, 2]. One aspect of this progress is the extension of the available wavelength coverage in the mid-infrared spectral range. Presently, a Type-I QC laser can be engineered to emit at wavelengths ranging from 4.5 to 24 μm. Most recently, a QC laser operating at $\lambda = 68$ μm was reported [3, 4], which represents the entry of semiconductor quantum emitters into the terahertz region. This extended spectral coverage opens wider opportunities for chemical sensing applications for QC lasers. For example, benzene can be detected most efficiently at a wavelength of 14.8 μm (674 cm^{-1}), where there is a strong narrow Q-branch of its ν_4 vibrational mode [5, 6].

Another achievement in QC laser engineering is the availability of lasers capable of operation at non-cryogenic temperatures, within the temperature range of thermoelectric coolers (TEC) [2, 7]. Such devices are especially attractive for portable spectroscopic gas sensors [8]. However, most thermoelectrically cooled QC lasers require a high current and must be driven in a pulsed mode at low duty cycle to prevent overheating of the active region. This mode of operation sets specific challenges for spectroscopic applications. Laser line broadening must be minimized, and a method for laser frequency tuning must be developed.

At longer wavelengths, the photodetector types that do not require cooling below liquid nitrogen temperatures are limited. Although HgCdTe photovoltaic detectors have their long cut-off wavelength at 11.5 μm, photoconductive detectors based on the same material can be used up to 22 μm, but require cryogenic cooling, which should be avoided in a portable gas sensor design. Therefore, we employed a thermal (pyroelectric) detector, which requires no cooling and has a flat response over a wide spectral range.

Spectroscopic measurements of CO_2 and H_2O concentrations present in ambient air were performed to evaluate the new signal detection and wavelength scanning techniques developed in this work for pulsed QC-DFB lasers operating at 15.6 μm. These approaches can be transferred and applied, for example, to volatile organic compounds (VOCs), in particular benzene detection with a 14.8-μm pulsed QC-DFB laser [6].

2 Experimental details

2.1 *General description*

The experimental set-up for the acquisition of spectroscopic data with a $\lambda = 15.6$ μm QC-DFB laser is shown in Fig. 1. The laser chip was mounted on a three-stage TEC inside an evacuated housing, described in [9, 10]. The output window of the laser housing was tilted 5° to suppress optical interference fringes caused by reflections from its surfaces. The pulsed laser driver (Directed Energy

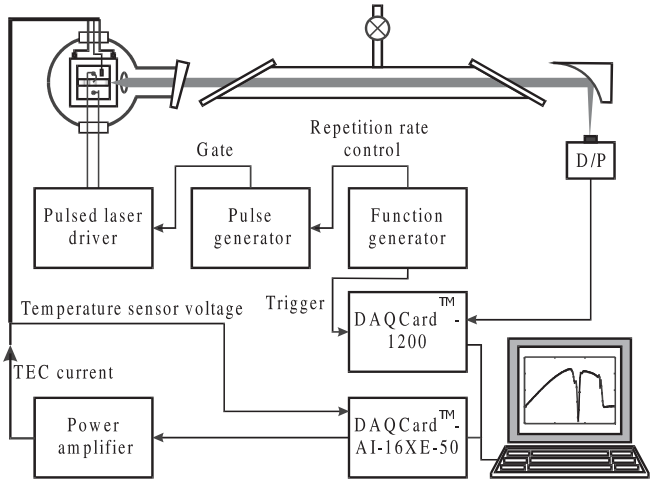

FIGURE 1 Experimental arrangement

✉ Fax: +1-713/348-5686, E-mail: akoster@rice.edu

Inc. DLD-100B) produced current pulses with the same duration as the TTL gate pulses, with a minimum pulse length of 14 ns. The gate pulses were generated by a locally built pulse generator. The pulse repetition rate was controlled by an external voltage. Two PCMCIA cards (National Instruments) were used with a laptop computer for laser temperature control and data acquisition. A DAQCard™-1200 was used exclusively for laser temperature control through a proportional-integral-derivative (PID) algorithm, while a DAQCard™-AI-16XE-50 card was used for data acquisition. A 45-cm-long single-pass gas cell equipped with ZnSe Brewster windows was employed in the spectroscopic measurements.

2.2 *Pyroelectric detection for long-wavelength mid-infrared gas sensors*

We used a pyroelectric detector (LIE 311f, InfraTec®) in a current mode with a Rice-developed preamplifier to detect the laser radiation. The responsivity of this detector varied $< 2\%$ in the spectral range from 1 to 17 μm and exhibited useful sensitivity to 25 μm according to the technical data. Our tests showed that the active area of the detector was circular, with an almost flat sensitivity profile of 1.2-mm diameter. The detector/transimpedence preamplifier bandwidth was measured to be 8 to 1150 Hz. At higher modulation frequencies, the response dropped at a rate of 4.25 dB/octave. The noise spectrum of this detector/preamplifier (D/P) acquired in the absence of laser radiation is shown in Fig. 2. When the QC laser radiation was applied, a number of peaks at various harmonics of the power line frequency (60 Hz) appeared. This noise was due to the line pickup converted to the laser power modulation. It can be avoided either by using a battery-powered laser driver or by the appropriate choice of modulation frequency. At 200 Hz, the D/P noise was 10^{-5} V in a 1 Hz band. The D/P sensitivity was calibrated using a 1.66-μm diode laser and power meter and found to be 3.84 V/mW. Thus, if the laser power is 0.1 mW and the modulation frequency is 200 Hz, the SNR in a 1 Hz band exceeds 38 000, which means that the detectable absorption is $< 3 \times 10^{-5}$. This performance is adequate for most gas-sensing applications.

3 Long-wavelength mid-infrared QC laser characterization

3.1 *Spectral properties, power and beam structure*

A QC-DFB laser chip designed for near-room-temperature operation in a low-duty cycle mode was fabricated at the University of Neuchâtel [11]. The chip originally contained two single-frequency lasers. Both devices were electrically similar to a 3 Ω resistor. Their tuning characteristics were initially obtained at the University of Neuchâtel using an FTIR spectrometer, and subsequently verified at Rice University by comparing the acquired absorption spectra of CO_2 with HITRAN-based simulations. The first laser (laser I) operated at approximately 646 cm^{-1} with a temperature tuning coefficient of $-0.053\,cm^{-1}/K$, and the second laser (laser II) at approximately 637 cm^{-1} with a temperature tuning coefficient of $-0.048\,cm^{-1}/K$. The lasing threshold for both devices was close to 7 A (10 kA/cm^2) at −40 °C, for current pulses of 50-ns duration at a 267-kHz pulse repetition rate. Both QC lasers operated up to +30 °C. Up to 18 A of peak current was applied to the lasers, which resulted in an average power of > 1 mW (Fig. 3) for the pulse durations and repetition rates given above. However, for spectroscopic measurements, the pulse duration and peak current were restricted to lower values in order to maintain a sufficiently narrow laser linewidth. In most of the experiments, the pulse duration was set to $\tau = 20$ ns and the peak current to $I \approx 10$ A. For such conditions and a laser temperature $T = -20$ °C, the maximum laser power detected after the absorption cell was 0.18 mW. The collimating lens and the

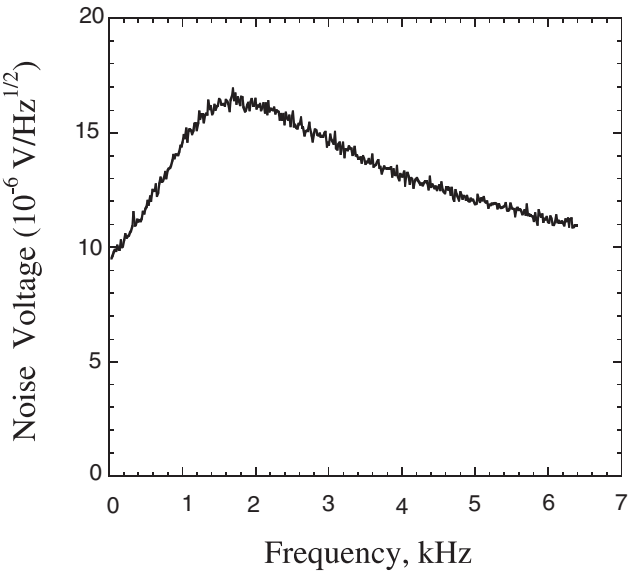

FIGURE 2 Noise spectrum of the pyroelectric detector with a locally built transimpedence preamplifier (D/P). The D/P sensitivity is 3.84 V/mW

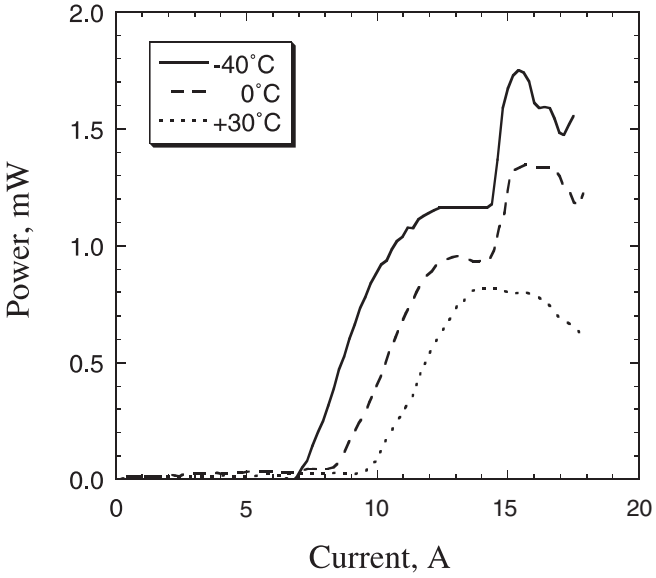

FIGURE 3 Laser power as a function of current for laser I. A sharp rise near 14 A marks the onset of multimode operation

laser housing window were ZnSe optics, AR coated for 8 to 12 μm and therefore introduced 17% combined power losses at 15.5 μm.

The aspherical collimating lens inside the laser housing, with a focal length of 3 mm, was aligned so as to provide the narrowest beam cross section at a distance of 40 cm from the laser housing window. This distance corresponded to approximately 55 cm from the lens. The resulting beam profile measured with the pyroelectric detector is shown in Fig. 4. No correction for a finite detector size was made.

We performed a series of experiments with laser I to establish the minimum laser linewidth. A 45-cm-long gas cell was filled with 1.3 Torr of CO_2. The laser was excited by a sequence of pulses with constant amplitude I, duration τ and repetition rate f, while the laser temperature was continuously varied from approximately $-20\,^{\circ}$C to $0\,^{\circ}$C to provide frequency tuning. The laser beam was mechanically chopped at 637 Hz. The observed CO_2 absorption lines were readily assigned and provided absolute frequency calibration. The laser frequency depended linearly on temperature, in agreement with earlier published results [12, 13]. The observed width of the CO_2 absorption line at 645.9407 cm^{-1} was compared for different values of I and τ. The best result with a FWHM $\Delta\nu_{exp} = 0.007\,cm^{-1}$ (210 MHz) is depicted in Fig. 5 along with the simulated absorption based on HITRAN'96 [14] data. This lineshape was obtained with $\tau = 17$ ns, $I = 9$ A ($\sim 5\%$ above threshold) and a 1 MHz pulse repetition rate. The average laser power reaching the detector was 17 μW. The theoretical FWHM of this partially saturated absorption line is $\Delta\nu_{th} = 0.002\,cm^{-1}$ (60 MHz). Both experimental and simulated lineshapes can be reasonably well fitted with a Gaussian function. Therefore, the QC laser linewidth can be estimated to be $\Delta\nu_l = [(\Delta\nu_{exp})^2 - (\Delta\nu_{th})^2]^{1/2} \approx 200$ MHz. An integration of the area under each curve shows good agreement between the theoretical and experimental data, confirming that the laser radiation is concentrated in a single laser mode. Spectral properties of laser II were similar to those of laser I. After completion of the linewidth optimization experiments, laser I was accidentally damaged, and all subsequent measurements described below were performed with laser II.

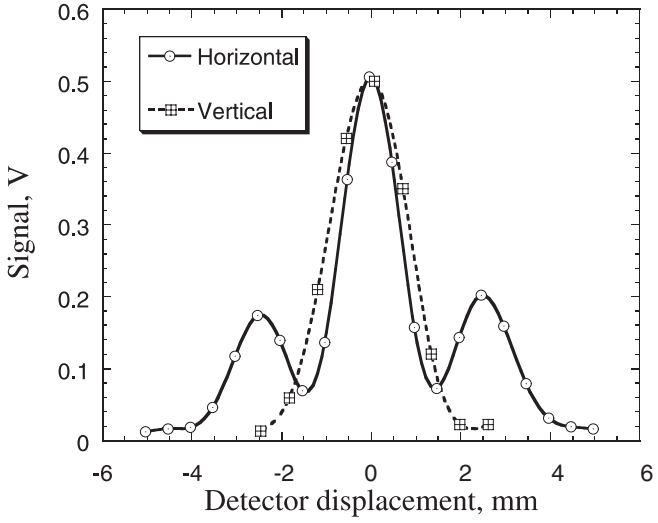

FIGURE 4 Spatial distribution of the laser power measured 55 cm from the collimating lens with a focal length of 3 mm. No correction for the detector size (1.2-mm-diameter active region) was made

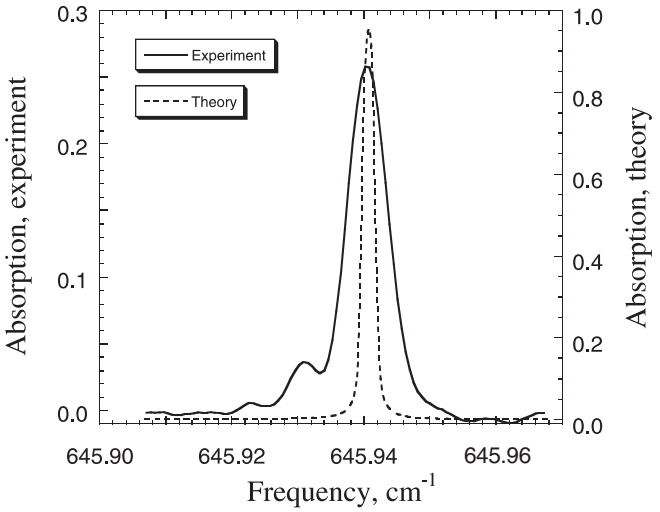

FIGURE 5 Minimum carbon dioxide absorption linewidth obtained compared with that calculated from HITRAN. The laser frequency was temperature-tuned and the laser beam chopped mechanically. The observed lineshape is clearly dominated by the QC laser spectral linewidth, yielding a laser line FWHM = 200 MHz

3.2 *Electronic chopping*

A pyroelectric detector requires modulated signals, since it does not respond to CW radiation. A mechanical optical chopper is convenient in laboratory operation, but not desirable in portable gas analyzers. We investigated the feasibility of electronic laser beam chopping (e-chopping): a train of nanosecond current pulses applied to the laser is switched ON and OFF at a certain frequency Ω. This scheme has the added advantage of reduced power consumption by both the laser and the TEC. We also found that the average laser power during ON periods was about 1.7-times higher compared to the mechanical chopping mode at the same peak pump current and laser wavelength. The laser wavelength was tuned, as previously, by changing the laser substrate temperature.

An e-chopped train of $\tau = 17$-ns-long, 9.5 A peak current pulses at 1 MHz repetition rate was applied to the QC-DFB laser. The absorption cell was filled with 10 Torr of CO_2 to explore the dependence of the spectrum upon chopping frequency. The acquired spectral data are shown in Fig. 6 along with the HITRAN simulated absorption spectrum. From Fig. 6 it is evident that the spectral resolution improves as the chopping frequency, Ω, decreases. From these data we conclude that when the train of current pulses is turned ON, an active area of the laser undergoes fast heating, resulting in a wavelength sweep. However, the laser linewidth at lower e-chopping frequencies remains narrow enough for spectroscopic gas sensing. At 200 Hz, the linewidth has a FWHM = $0.013\,cm^{-1}$, which is much less than the typical width of a ro-vibrational absorption line at atmospheric pressure ($\sim 0.1\,cm^{-1}$). The similarity of the spectra at $\Omega = 500$ Hz and 200 Hz indicates that for ON times of 1 ms or longer, the laser stays at its steady-state temperature during

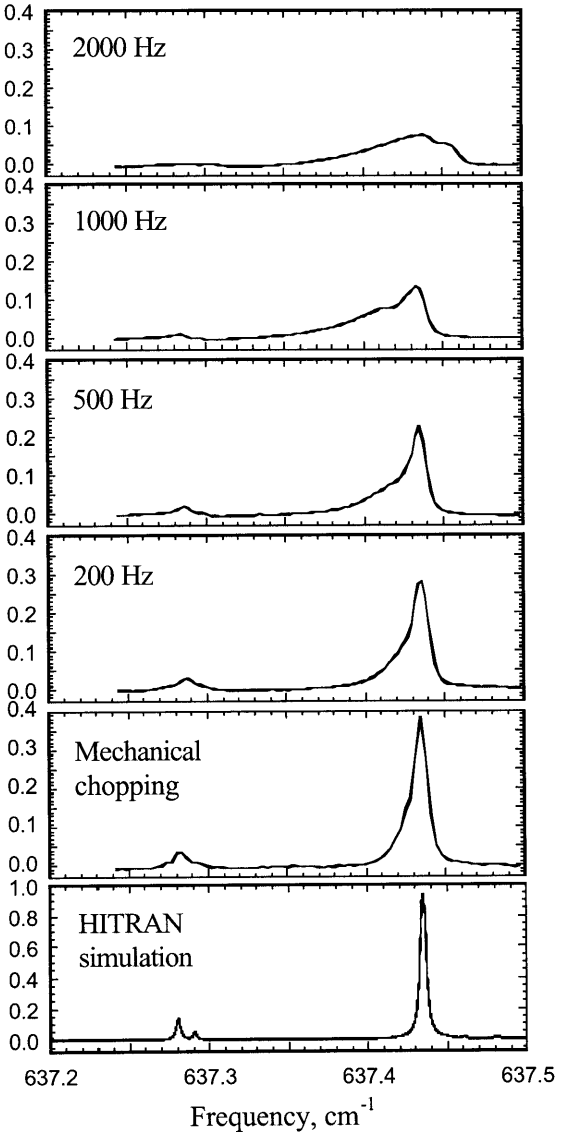

FIGURE 6 The observed CO_2 absorption line profile as a function of e-chopping frequency along with the same part of the CO_2 spectrum acquired with mechanical chopping of the laser beam and simulated with HITRAN

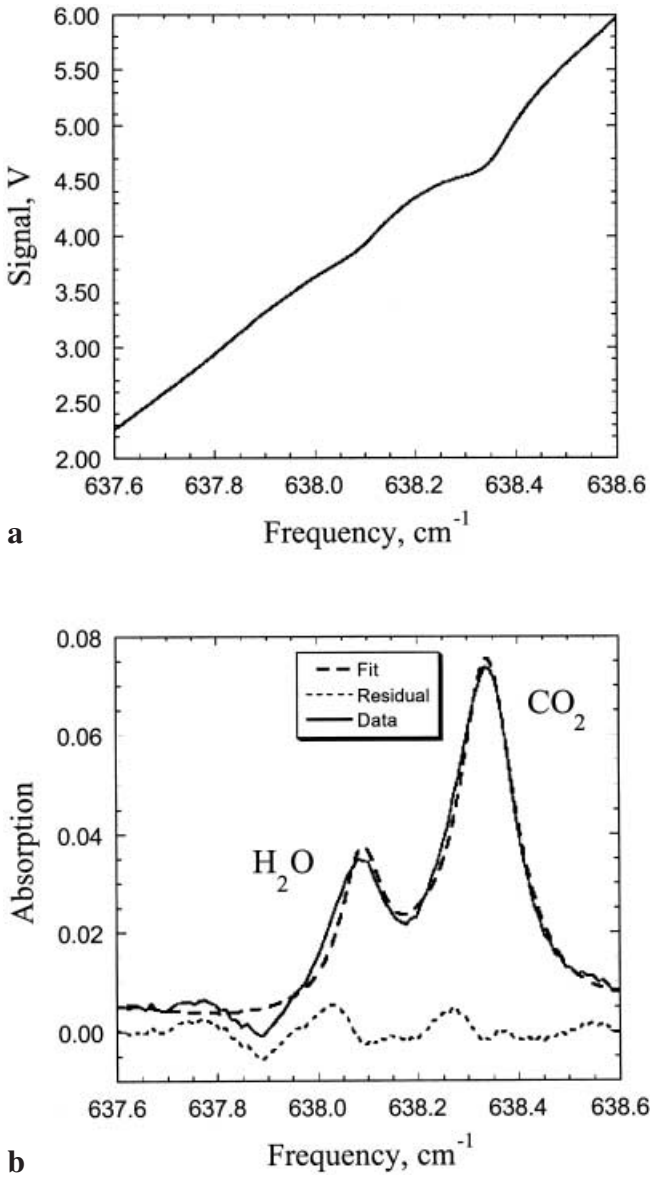

FIGURE 7 **a** The detected laser power (signal from a lock-in amplifier output) 59 cm from the laser housing window. The two dips correspond to absorption lines of CO_2 (stronger) and H_2O. The laser was temperature-tuned, and the frequency scale was defined using a position of the CO_2 absorption line and a previously obtained frequency vs temperature tuning coefficient (see Sect. 3.1). **b** CO_2 and H_2O absorption derived from the above set of data as described in Sect. 4.1

most of its ON time. The traces in Fig. 6 imply that the wavelength, and thus the temperature, settling time was more than 0.5 ms and less than 1 ms.

4 CO_2 and H_2O concentration measurements in ambient air

4.1 *Slow wavelength scans by temperature tuning*

Figure 7a represents the laser power detected by the pyroelectric detector at a distance of 59 cm from the laser housing window, with the gas cell removed. The laser was e-chopped at 153 Hz and pumped by $I = 9.15$ A, $\tau = 17$ ns pulses. The D/P signal was acquired using a lock-in amplifier with a time constant set to 30 ms. The two dips on this curve are due to absorption by CO_2 and H_2O in ambient air. The detected signal S can be decomposed as follows:

$$S(\nu) = P_n(\nu)\ [1 - k_1 g_1(\nu) - k_2 g_2(\nu) + r(\nu)]\ , \qquad (1)$$

where ν is the optical laser frequency and $P_n(\nu)$ gives the laser power approximated by an n-th order polynomial. The power depends directly on the laser temperature T and indirectly on ν, via the relation $\nu = f(T)$. Functions $g_i(\nu)$, $i = 1, 2$, describe the absorption by CO_2 and H_2O, respectively. It was established that the primary absorption peaks were the 638.3394 cm^{-1} CO_2 line (P(38) of the fundamental ν_2 mode) and the 638.0891 cm^{-1} H_2O line (pure rotational band, $7_{7,0} \leftarrow 6_{4,3}$ transition). We simulated these functions using HITRAN-PC software with a subsequent convolution with the laser lineshape. The finite laser lineshape was responsible for a 5%–6% decrease in the height of each absorption line. The conditions selected were:

$g_1(\nu)$ – 330 ppm CO_2, 1 atm total pressure, 65 cm path length;
$g_2(\nu)$ – 10 Torr H_2O ($\sim$ 50% humidity at +20 °C), 1 atm total pressure, 65 cm path length.

Coefficients k_i relate the concentrations in the tested sample to the concentrations assumed in $g_i(\nu)$ simulations. The function $r(\nu)$ is the fit residual due to noise of different origin (laser and detector noise, mechanical vibrations, fluctuations of absorbing species in the moving air during the slow temperature scan) and unintentional interference fringes from optical elements.

The results of experimental data decomposition following (1) with $n = 3$ are shown in Fig. 7b. It depicts the absorption fit $k_1 g_1(\nu) - k_2 g_2(\nu)$ together with the residual $r(\nu)$. The best-fit coefficients are: $k_1 = 1.15$ and $k_2 = 0.80$, that is $[CO_2] = 380$ ppb and H_2O partial pressure 8 Torr (40% humidity).

4.2 *Fast wavelength scans by repetition rate modulation*

For many applications it is preferable to scan the laser temperature electronically (i.e. by some kind of laser current manipulation) rather than by changing the substrate temperature [9]. Temperature scans are intrinsically slow, and there is always some lag between the temperature sensor readings and the actual temperature of the laser active region, complicating the processing of spectral data. A common technique for fast-scanning of the pulsed QC-DFB laser wavelength is to apply a modulated (usually as a triangular ramp) sub-threshold current in addition to short intense pulses [15]. This technique works well if the average power dissipation resulting from the train of nanosecond pulses is small. This is not the case for the 15.6-μm laser used in this work and operated with a close to 1-MHz pulse repetition rate. With $I \sim 10$ A and a resistivity $R \sim 3$–$4\ \Omega$, the peak power dissipation exceeded 300 W, which resulted in 3 W or more of average dissipation at a 1% duty cycle. This generated a significant load to the TEC, and it was not desirable to further increase this load by adding a sub-threshold QC laser current. Furthermore, the laser exhibited a low temperature tuning coefficient. We have observed that an on–off modulated sub-threshold current of up to 280 mA ($\sim$ 1 W of additional power dissipation) did not result in noticeable laser line splitting.

A possible scheme to address this issue is to modulate the peak current of the short pulses in direct analogy to the way the wavelength of CW QC-DFB or diode lasers is normally scanned. However, this approach has a significant shortcoming; the linewidth and spectral shape of the pulsed QC-DFB laser emission strongly depends on the pump current, unlike the case for CW operation.

We developed a technique for fast scanning of the pulsed laser wavelength by modulating the repetition rate f of the laser pulses. In this case, the thermal dissipation in the laser was directly proportional to the control voltage V_f applied to a voltage-to-frequency converter. The repetition rate was linearly swept from 100 kHz to 1000 kHz in about 11 ms, as shown in Fig. 8, followed by an off period of the same duration to allow the pyroelectric detector to relax. It can be seen that in this mode, the average laser power grows until 810 kHz of the repetition rate followed by a roll-off because of the laser heating. The peak detector signal corresponds to a laser power of 130 μW. In this case, the pulse duration and current were set to $\tau = 20$ ns and $I = 9.5$ A, respectively. These values were chosen to satisfy a compromise between the wavelength-scan span and the laser linewidth (both grow with a per-pulse dissipation $W \sim \tau I^2$).

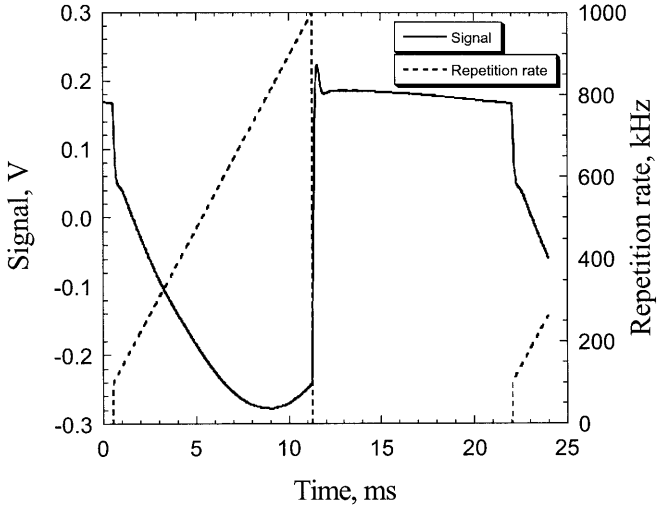

FIGURE 8 Fast sweep of the laser-pulse repetition rate: signal detected by D/P and the repetition rate versus time

An absolute calibration of the laser frequency for fast wavelength scans was performed using CO_2 absorption lines in the same way as for the temperature scans. For a detailed relative frequency calibration we used interference fringes created by two air-separated uncoated ZnSe surfaces. The results shown in Fig. 9a and b confirm that the optical frequency versus repetition rate dependence is close to linear. The deviation from linearity is less than $\pm 0.006\ cm^{-1}$ over the entire 0.6-cm^{-1} scan.

In order to measure atmospheric concentrations of H_2O and CO_2, a 45-cm-long gas cell placed in the QC-DFB laser-beam path was initially evacuated and then filled with air at atmospheric pressure. These two data sets were used to obtain the absorption spectrum of ambient air shown in Fig. 10. This spectrum was fitted by the function

$$A(\nu) = k_1 h_1(\nu) + k_2 h_2(\nu), \tag{2}$$

where the functions $h_i(\nu)$, $i = 1, 2$ represent absorption by CO_2 and H_2O, respectively, simulated using HITRAN-PC at the same conditions as functions $g_i(\nu)$ in Sect. 4.1 but with a 45-cm-path and then convolved with an instrument function. The instrument function is shown as an insert in Fig. 10 and was obtained by acquiring a CO_2 absorption spectrum at low pressure with subsequent smoothing. The dashed and dotted curves in Fig. 10 show the functions $k_i g_i(\nu)$ with the best-fit coefficients, which correspond to a CO_2 concentration of 465 ppm and a H_2O partial pressure of 5.1 Torr (25% humidity at +22 °C). The fit residual is much less than that of the slow scan (compare to Fig. 7b). This is probably due to the absence of the influence of slow drifts caused, for example, by laboratory personnel who constantly move and exhale air containing 4%–5% of CO_2 enriched with H_2O vapor. Hence, the fast wavelenght scan method provides more reliable absorption data.

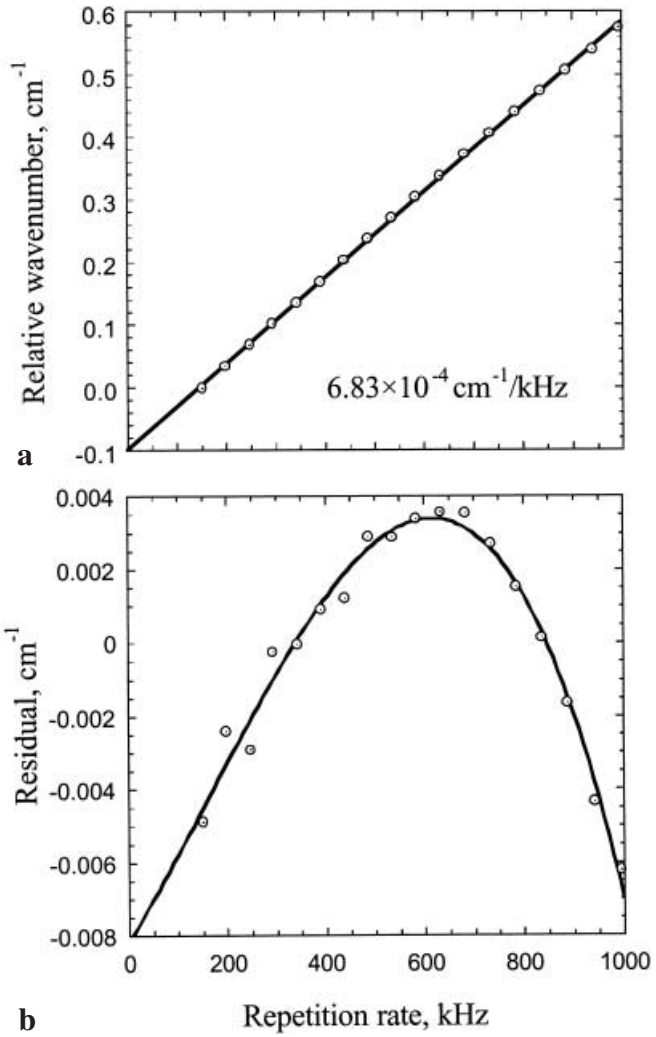

FIGURE 9 **a** Positions of interference fringes from two air-spaced ZnSe surfaces versus the laser current pulse repetition rate. The fast repetition rate sweep is performed for the same conditions as the sweep shown in Fig. 8. The vertical scale is based on a separation $d = 14.8$ cm of the ZnSe surfaces, which yields FSR $= 1/(2d) = 3.38 \times 10^{-2}$ cm^{-1}. **b** Deviations of the above positions from the linear fit along with a best 3rd-order polynomial fit

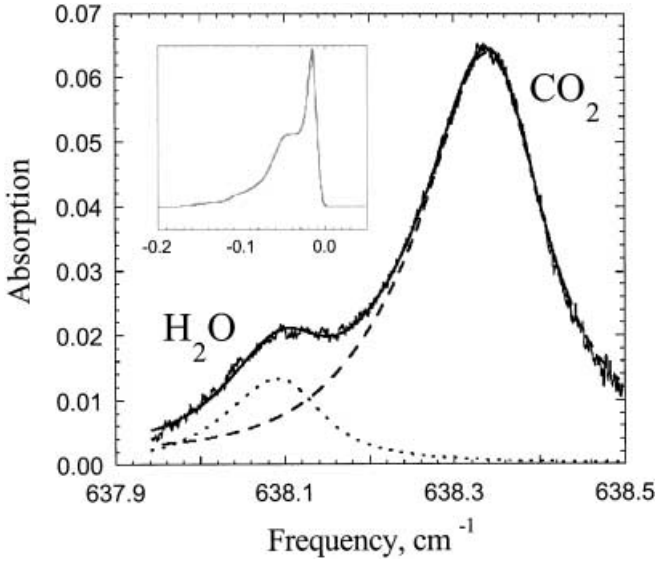

FIGURE 10 Water and carbon dioxide absorption lines in the laboratory atmosphere. Data was acquired using the fast scan technique. The line exhibiting noise is the experimental absorption. The *heavy solid line* is a fit of the absorption with two adjustable parameters, the peak intensities of the two lines, and the *dashed curves* are contributions to the absorption from each line. An *insert* shows the spectral lineshape of the laser, horizontal scale in cm^{-1}

In order to estimate the effect of pyroelectric detector noise on the data presented in Fig. 10, we assumed a data acquisition card bandwidth 66 kHz, as specified by its manufacturer from its specifications, at a gain of 10. Since each of the two data sets used to obtain the absorption spectrum is a result of the averaging of 100 scans, the bandwidth is reduced to 660 Hz. The D/P noise density at this frequency is $13\,\mu\text{V/Hz}^{1/2}$. Subtraction of the one data set from the other increases the noise $\sqrt{2}$-times. Thus, the expected noise is $13\frac{\mu\text{V}}{\sqrt{\text{Hz}}} \times \sqrt{660\,\text{Hz}} \times \sqrt{2} = 470\,\mu\text{V}$. Taking into account that the maximum D/P signal was approximately 470 mV, we obtain SNR = 1000. In other words, the D/P related point-to-point noise in the absorption spectrum should be approximately 10^{-3}. This value is in a good agreement with what is observed in Fig. 10.

The CO_2 concentration values obtained are reasonable for both the slow and fast methods of wavelength tuning (the experiments were separated by approximately 5 months), but the calculated humidity seems to be too low. Typical hygrometer readings in the laboratory were in the 60 to 70% range. We double-checked the fast scan data by acquiring absorption spectra at 240 Torr of air in the cell, when the absorption lines of CO_2 and H_2O were virtually separated. The area under the H_2O line was calculated from the experimental data and then compared to HITRAN-based simulations. This procedure resulted in a 4.9 Torr of H_2O partial pressure, in a good agreement with the 5.1 Torr found previously. We believe that this discrepancy with the hygrometer readings indicates an inaccuracy in the HITRAN'96 data with respect to this particular rotational H_2O band.

5 Conclusions

We have demonstrated that a pulsed QC-DFB laser operating in the spectral region beyond 10 μm can be used in combination with a low-cost pyroelectric detector for sensitive absorption spectroscopy. This detector is suitable for achieving a $< 0.003\%$ absorption detectivity in a 1-Hz bandwidth with 0.1 mW of laser power. The novel technique of scanning the optical laser frequency by varying the repetition rate of the QC laser current pulses was demonstrated and provides a convenient means for performing fast wavelength scans. This method can potentially be used to modulate laser wavelengths at frequencies of up to several kHz. CO_2 and H_2O concentration measurements in ambient air were performed. Water vapor concentrations were monitored using a rotational absorption line. To the best of our knowledge, this represents the first observation of a pure rotational line obtained with a QC laser.

ACKNOWLEDGEMENTS Financial support of the work performed by the Rice group was provided by the National Aeronautics and Space Administration (NASA), Institute for Space Systems Operations (ISSO), the Texas Advanced Technology Program, the National Science

Foundation and the Welch Foundation. The work performed at the University of Neuchatel, Switzerland, was partially supported by the Swiss National Science Foundation.

REFERENCES

1 J. Faist, F. Capasso, D.L. Sivco, C. Sirtori, A.L. Hutchinson, A.Y. Cho: Science **264**, 553 (1994)
2 F. Capasso, C. Gmachl, R. Paiella, A. Tredicucci, A.L. Hutchinson, D.L. Sivco, J.N. Baillargeon, A.Y. Cho: IEEE Sel. Top. Quant. Electron. **6**, 931 (2000)
3 M. Rochat, L. Ajili, H. Willenberg, J. Faist, H. Beere, G. Davies, E. Linfield, D. Ritchie: Appl. Phys. Lett. (2002) submitted
4 R. Köhler, A. Tredicucci, F. Beltram, H.E. Beere, E.H. Linfield, A.G. Davies, D.A. Ritchie, R.C. Lott: Nature **417**, 156 (2002)
5 W. Chen, F. Cazier, F.K. Tittel, D. Boucher: Appl. Opt. **39**, 6238 (2000)
6 Environmental Protection Agency of US, Fourier Transform Infrared (FTIR) Reference Spectra, http://www.epa.gov/ttn/emc/ftir/refnam.html
7 D. Hofstetter, M. Beck, T. Aellen, J. Faist, U. Oesterle, M. Ilegems, E. Gini, H. Melchior: Appl. Phys. Lett **78**, 1964 (2001)
8 A.A. Kosterev, F.K. Tittel: IEEE J. Quantum Electron. **QE-38**, 582 (2002)
9 A.A. Kosterev, R.F. Curl, F.K. Tittel, R. Köhler, C. Gmachl, F. Capasso, D.L. Sivco, A.Y. Cho: Appl. Opt. **41**, 573 (2002)
10 A.A. Kosterev, R.F. Curl, F.K. Tittel, R. Köhler, C. Gmachl, F. Capasso, D.L. Sivco, A.Y. Cho, S. Wehe, M. Allen: Appl. Opt. **41**, 1169 (2002)
11 M. Rochat, M. Beck, J. Faist: Appl. Phys. Lett. **79**, 4271 (2001)
12 R. Köhler, C. Gmachl, F. Capasso, A. Tredicucci, D.L. Sivco, A.Y. Cho: IEEE Photonics Tech. Lett. **12**, 474 (2000)
13 A.A. Kosterev, F.K. Tittel, C. Gmachl, F. Capasso, D.L. Sivco, J.N. Baillargeon, A.L. Hutchinson, A.Y. Cho: Appl. Opt. **39**, 6866 (2000)
14 L.S. Rothman, C.P. Rinsland, A. Goldman, S.T. Massie, D.P. Edwards, J.M. Flaud, A. Perrin, C. Camy-Peyret, V. Dana, J.Y. Mandin, J. Schroeder, A. McCann, R.R. Gamache, R.B. Wattson, K. Yoshino, K.V. Chance, K.W. Jucks, L.R. Brown,V. Nemtchinov, P. Varanasi: J. Quant. Spectrosc. Radiat. Transfer **60**, 665 (1998)
15 S.W. Sharpe, J.F. Kelly, J.S. Hartman, C. Gmachl, F. Capasso, D.L. Sivco, J.N. Baillargeon, A.Y. Cho: Opt. Lett. **23**, 1396 (1998)